sciendo

VOLUME 18, N° 2 2024
Journal of Automation, Mobile Robotics and Intelligent Systems

# Design of Small-phase Time-Variant Low-pass Digital Fractional Differentiators and Integrators

Submitted: 3rd October 2023; accepted: 8th February 2024

*Mateusz Saków*

DOI: 10.14313/JAMRIS/2-2024/15

**Abstract:**
*The design method and the time-variant finite impulse response (FIR) architecture for real-time estimation of fractional and integer differentials and integrals are presented in this paper. The proposed FIR architecture is divided into two parts. Small-phase filtering, integer differentiation, and fractional differential and integration on the local data are performed by the first part, which is time-invariant. The second part, which is time-variant, handles fractional and global differentiation and integration. The separation of the two parts is necessary because real-time matrix inversion or an extensive analytical solution, which can be computationally intensive for high-order FIR architectures, would be required by a single time-variant FIR architecture. However, matrix inversion is used in the design method to achieve negligible delay in the filtered, differentiated, and integrated signals. The optimum output obtained by the method of least squares results in the negligible delay. The experimental results show that fractional and integer differentiation and integration can be performed by the proposed solution, although the fractional differentiation and integration process is sensitive to the noise and limited resolution of the measurements. In systems that require closed-loop control, disturbance observation, and real-time identification of model parameters, this solution can be implemented.*

**Keywords:** *fractional differentiation, fractional integration, FIR filter, digital filter synthesis*

## 1. Introduction

The fractional-order calculus has a widespread potential for application. Currently, this complex mathematical operator benefits the modelling of biological, chemical, control, electrical, and even financial systems [1–23]. However, the practical implementation of the fractional-order calculus is extremely difficult due to the lack of real components that can realize this mathematical operation [5, 24–28]. In the case of the integer differentiation and integration, passive electrical components such as capacitors and coils can carry out these operations on the analogue signal [29]. Moreover, the digital representation of the real-time integer-order calculus is also trivial and addressed by existing solutions and scientific papers [4, 5, 30–33].

However, there are no robust passive components capable of realizing the generalized arbitrary order of the fractional calculus, which allows for more accurate and real-time control, modelling, and simulation of the real systems [4, 5].

The literature [4, 5], presents three common mathematical definitions of the arbitrary-order derivative and integral proposed by Riemann–Liouville, Grünwald–Letnikov, and Caputo [1–5]. These mathematical definitions can be implemented by using the time-domain [4, 5, 34–36], and frequency-domain design methods [4, 5]. One of the frequency-domain design methods is Oustaloup's approximation, which is based on a recursive distribution of zeros and poles into a frequency interval [37]. This method was refined to achieve a better fit in the frequency response in [38]. Another design method is based on Charef's approximation, which has two versions. The first version approximates a function of singularities of poles and zeros within a limited frequency bandwidth with respect to a defined approximation error [39], while the second version extends the Charef method by including additional arbitrary poles [39]. The next design method is Carlson's approximation method [40], which is based on the Newton iterative root-finding algorithm. Moreover, there are noniterative design methods, such as Matsuda's approximation, where a set of logarithmically spaced frequencies is used to approximate the ideal fractional-order function [41]; and the continued fraction expansion approximation, which is also used for evaluation of the fractional-order functions because it converges faster than power series expansions [42]. Matsuda's approximation method was also refined in [43, 44], by applying the Sanathanan–Koerner least-squares method [45]. A further refinement of Matsuda's method is the modified stability boundary locus fitting approximation [27, 46], which is based on an additional closed-loop system composed by a proportional-integral controller.

More frequency-domain approximation methods can be found in the literature, such as the Fourier series and inverse Fourier transform method [34], vector fitting method [47], Abdelbaki's method [48], Maione's approximation [49], and Thiele's approximation [50]. In all these cases, however, the ideal transfer function of a fractional differentiator or integrator is approximated by an integer-order rational transition function through the pole-zero pairs.

Therefore, the integer-order rational transition function can be synthesized with passive analogue components or implemented into a digital real-time system. Nevertheless, the approximation can be valid only for a limited number of fractional orders and the difference between the responses of the ideal transfer function and its approximation is unknown [4,5]. Furthermore, all the frequency-domain design methods provide only approximation in a limited frequency bandwidth, thus, they give less importance to the parts of the frequency response in the borders and outside of this bandwidth. Hence, in the low-pass filter design case, this results in poor approximation in the passband frequency and poor attenuation for the stopband frequency, and/or amplification in the stopband frequency spectrum [4,5].

The frequency-domain design methods can be adapted to digital architectures, such as the infinite impulse response (IIR) and the finite impulse response (FIR) filters [5, 51]. To adapt continuous transfer functions to their discrete equivalents, two types of discretization methods can be used [52–58], the direct [53, 54] and the indirect discretization [59, 60]. Moreover, there are methods that were introduced to design both the integer differentiators and integrators [61–69]. In the case of integer-order design methods, the transfer function of a digital integrator (based on the rectangular rule) can be inverted and stabilized to obtain the IIR differentiator [61]. A similar design approach was presented in [62, 63], where the integrator is obtained by combining both the rectangular and trapezoidal techniques. In this case, the differentiator is also obtained by inverting and stabilizing the integrator transfer function. An alternative design method was presented in [64], where the digital integrator is designed with respect to the Simpson integration rule, and the differentiator is obtained again by inverting the integrator transfer function. Another design method is based on the closed-form Newton-Cotes integration formula [68], where the third-order digital trapezoidal integrator is obtained and inverted to form the differentiator. Another solution was proposed in [70], where the adaptation of the method of least squares was used to design the integer FIR differentiator. Furthermore, alternative methods are the Adomian decomposition method [71], the Chebyshev collocation method [72, 73], and the predictor–corrector approach based on the Adams–Bashforth–Moulton method [74–76]. Nevertheless, these three methods are not robust enough to be implemented in a real-time system, and are therefore limited to numerical simulations only [4,5].

The direct and indirect discretization methods lead to a discrete transfer function, which has the same drawbacks as the transfer function designed with respect to the frequency-domain design methods. Hence, only the FIR and IIR integer differentiators and integrators can estimate their output with respect to the close-to-ideal magnitude response. However, only one solution allows designing the integer FIR differentiator that is characterized by a negligible phase shift in the passband frequency and significant attenuation in the stopband frequency spectrum [70]. Other solutions [61–69] are characterized by linear or nonlinear phase responses, which lead to a time delay in the differentiated and integrated signals or imprecise response with respect to (periodic) signals with varying frequency. This, in turn, limits their applications in closed-loop control and real-time estimation and recovery of the state variables in, e.g., disturbance observer design [77–85].

In this paper, the time-variant FIR architecture and its design method for real-time local and global fractional and integer differentiation and integration are presented. The proposed FIR architecture is divided into two parts. Small delay (small-phase shift) filtering, integer differentiation, and potentially local fractional differentiation and integration are performed by the first part, which is time-invariant. This part is based on the previously introduced FIR filter and integer differentiator architectures presented in [70], and is also extended to the fractional-order calculus in this paper. Fractional (global) differentiation and integration are performed by the second part, which is time-variant. The separation of the two parts is necessary because real-time matrix inversion or extensive analytical solutions, which can be computationally demanding for high-order FIR architectures, are required by the time-variant FIR architecture. Moreover, matrix inversion is used in the design method to ensure small delay introduced into the filtered, differentiated, and integrated signals by both parts of the FIR architectures. The optimum output obtained by the method of least squares results in the negligible phase shift introduced by the FIR architecture.

This paper is organized as follows: Section 2 describes the problems regarding the implementation of the fractional differentiators and integrators; Section 3 introduces the time-variant FIR architecture and its design method; Section 4 discusses the experimental results; and Section 5 concludes the paper.

## 2. Problem Statement

The fractional derivative (integral) [1–5, 51] of the power function $f(t) = t^p$ is given by:

$$D^v t^p = \frac{\Gamma(p+1)}{\Gamma(p-v+1)} t^{p-v}, \tag{1}$$

where the integer order $q$ of the integer derivative (integral) is generalized to an arbitrary order $v$ by replacing $p!$ and $(p-q)!$ with gamma functions $\Gamma(p+1)$ and $\Gamma(p-v+1)$, respectively. If $p-v+1 > 0$, the gamma function $\Gamma(p-v+1)$ [1–5,51] can be computed as follows:

$$\Gamma(p-v+1) = \int_0^\infty x^{p-v} e^{-x} dx. \tag{2}$$

Furthermore, if $p - v + 1 \leq 0$, the gamma function $\Gamma(-x)$ can be computed by using the reflection property of the gamma function as follows:

$$\Gamma(-x) = \frac{-\pi \csc(\pi x)}{\Gamma(x+1)}. \tag{3}$$

Based on (1) with respect to (2) and (3), the fractional derivative (integral) of a given function $f(t)$ transformed into a polynomial of $t$ by using Taylor series expansion is given by:

$$D^v f(t) = \sum_{p=0}^{\infty} a_p \frac{\Gamma(p+1)}{\Gamma(p-v+1)} t^{p-v}, \tag{4}$$

where $a_p$ is the $p^{th}$ coefficient of the given polynomial. The problem in this case is that the transfer function of the FIR architecture (filter, differentiator, or integrator) described by:

$$H(z) = \sum_{k=0}^{N} h(k) z^{-k}, \tag{5}$$

where $z$ is the $z$-transform and $N$ is the order of the FIR architecture, must calculate the combined differentiated and integrated output. Unfortunately, the FIR architecture does not store and use data outside the limited data set (local samples of the modified signal) used to calculate the output of that FIR architecture. Therefore, the FIR architecture does not include time base, and it cannot estimate both the global integer integrals and the fractional order differentials/integrals.

## 3. Time-variant FIR Architecture and Its Design

The proposed time-variant FIR architecture, designed according to the proposed design method, consists of two separate parts. Both parts are shown in Figure 1.

The first and second parts of the FIR architecture are designed separately. The first part performs filtering, integer and local fractional differentiation and integration. When the first part is designed as a low-pass FIR filter, the second part can act as both an integer- and fractional-order differentiator and integrator.

Both FIR architectures consist of delay lines built from unitary delays $z^{-1}$, which create $N_f$ consecutive delayed signals from the input signal $x[n]$. The first architecture consists of gains $W_f(N_f)$ and the sum blocks Σ. The second FIR architecture uses a multiplexer (MUX) to obtain $N_m$ signals from the delay line. These signals are multiplied by matrices $W_m(t)$ and $L_m(t)$ to obtain the resulting output $y[n]$.

The first part is designed according to the algorithm presented in [70], which was developed to design small-phase FIR filters and integer-order differentiators. However, in this work, two modifications to the time sample vector of the FIR architecture $Y_f$ are introduced. The time sample vector is described as follows:

$$Y_f = [1-d, 1+\Delta t-d, \ldots, 1+(N_f-1)\Delta t-d, N_f\Delta t-d]^T, \tag{6}$$

where $N_f \in \mathbb{N}$ is the order of the first FIR architecture and $T$ stands for transpose operator.

The first modification introduces the sampling period $\Delta t$ in (6). This modification eliminates the need for the gain scaling factor $(-1/\Delta t)^{v_f}$, where $v_f$ is the order of fractional derivative/integral. The scaling factor was required in [70] to adjust the gain of the FIR differentiator with respect to the sampling rate. In (6), the scaling factor is eliminated because it becomes a complex number for fractional differentials and integrals.

The second modification allows designing a time delay $d$ introduced by the first FIR architecture. The purpose of designing the time delay is to increase the attenuation of the stopband frequency. The FIR filter and integer differentiator designed with respect to [70] minimizes the phase shift and attenuation of the stopband frequency by estimating the output of the FIR architecture, which is optimal with respect to the method of least squares. The introduction of the time delay allows the output of the FIR architecture to be calculated with respect to the samples surrounding the filtered sample of the signal instead of filtering that sample based on only the past samples [70].

The time sample vector (6) is used to create the following matrix:

$$X_f = [Y_f^0, Y_f^1, \ldots, Y_f^{p_f-1}, Y_f^{p_f}], \tag{7}$$

where $p_f \in \mathbb{N}$ corresponds to the order of a theoretical polynomial fitted by the FIR architecture. The weights of this FIR architecture are calculated as follows:

$$W_f = L_f((X_f^T X_f)^{-1} X_f), \tag{8}$$

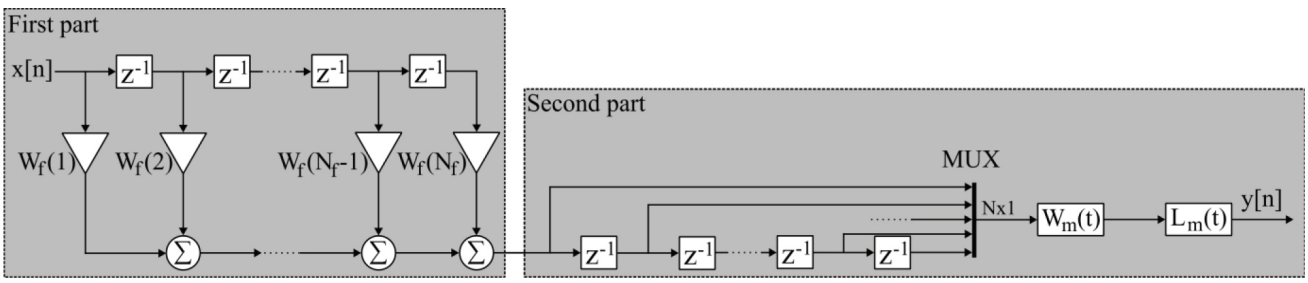


**Figure 1.** FIR architecture for real-time integer- and fractional-order differentiation and integration

where

$$L_f = \left[\frac{\Gamma(1)}{\Gamma(1-v_f)}, \frac{\Gamma(2)}{\Gamma(2-v_f)}, \dots, \frac{\Gamma(p_f)}{\Gamma(p_f-v_f)}, \frac{\Gamma(p_f+1)}{\Gamma(p_f-v_f+1)}\right], \quad (9)$$

where $L_f$ is the vector of weights transforming the left-sided Moore–Penrose generalized inverse solution in (8) to the FIR architecture weights $W_f(N_f)$. The $L_f$ vector is generalized to an arbitrary order of the fitted polynomial $p_f$, and fractional-order of the derivative/integral $v_f$ in the gamma function $\Gamma(p_f, v_f)$.

The first FIR architecture can be used to filter, differentiate, and integrate the signal $x[n]$. However, the output $y[n]$ will correspond only to the local (fractional) differentials and integrals at the point with respect to the time sample vector (6). To solve this problem, the additional time-variant FIR architecture was introduced.

In the second FIR architecture, all the parameters are time-dependent. Therefore, the time sample vector $Y_m(t)$ of the second FIR architecture includes time-base $t$, and is described as follows:

$$Y_m(t) = [t, t-\Delta t, t-2\Delta t, \dots, t-(N_m-2)\Delta t, t-(N_m-1)\Delta t]^T, \quad (10)$$

where $N_m \in \mathbb{N}$ corresponds to the order of a theoretical polynomial, fitted again by the time-variant FIR architecture. In (10) there is no need to introduce the delay because filtering is left to the first FIR architecture. Based on (10), the time-dependent matrix $X_m(t)$ is described as follows:

$$X_m(t) = [Y_m^0(t), Y_m^1(t), \dots, Y_m^{p_m-1}(t), Y_m^{p_m}(t)], \quad (11)$$

where $p_m \in \mathbb{N}$ corresponds to the order of the fitted polynomial in the second FIR architecture. Then, (11) is used to obtain the weights of the second FIR architecture as follows:

$$W_m(t) = L_m(t)((X_m^T(t)X_m(t))^{-1}X_m(t)), \quad (12)$$

where

$$L_m(t) = \left[\frac{\Gamma(1)}{\Gamma(1-v_m)}t^{-v_m}, \frac{\Gamma(2)}{\Gamma(2-v_m)}t^{1-v_m}, \dots, \frac{\Gamma(p_m)}{\Gamma(p_m-v_m)}t^{p_m-1-v_m}, \frac{\Gamma(p_m+1)}{\Gamma(p_m-v_m+1)}t^{p_m-v_m}\right], \quad (13)$$

where $L_m(t)$ is again the time-dependent vector of weights transforming the left-sided Moore–Penrose generalized inverse solution in (12) to the FIR differentiator and integrator weights $W_m(t)$. The $L_m(t)$ vector is also generalized to an arbitrary order fitted polynomial $p_m$, and fractional-order of the derivative and integral $v_m$ in the gamma function $\Gamma(p_m, v_m)$. Furthermore, (8) includes the time base which is defined as the power functions $t^{(p_m-v_m)}$.

The entire FIR architecture (Fig. 1) was divided into two parts because a single time-variant FIR architecture designed according to (10)–(13) requires real-time matrix inversion or an analytical solution of (12). In this case, matrix inversion of (12) can be computationally intensive, especially, for high-order FIR architectures.

Therefore, the entire FIR architecture structure was divided into the time-invariant and time-variant parts, where in the case of the time-variant part, the order of FIR structure can be as low as possible ($N_f > p_f$) and ($N_m > p_m$), because the filtering process is left to the first part. Furthermore, $W_m(t)$ consists of only $N_m^2$ parameters, thus, the differentiation and integration order can be updated in real-time without the need to recalculate the parameters of the entire FIR architecture.

There are two main limitations of the proposed solution. The first limitation comes from the ability to approximate input signal $x[n]$ by the time-variant FIR architecture. If the order of the polynomial $p_m$ is lower than the theoretical order of the polynomial approximating input signal $x[n]$, the error between output $y[n]$ and theoretical integer integral and fractional-derivatives and fractional-integrals approximating $x[n]$ will increase as the difference increases between orders of polynomials. Moreover, analytical solution of (12) leads to mathematical expressions such as $t(p_m)+\Delta t(p_m)$. In this case, if $t \gg \Delta t$, numerical errors will appear after numerical accuracy is reached during calculation of $t(p_m) + \Delta t(p_m)$. Furthermore, differentiator or integrator designed according to proposed method will estimate its output with respect to zero initial conditions. Nevertheless, despite these limitations, there are systems oriented on closed-loop control, disturbance observations and real-time identification of model parameters, where proposed solution can be implemented.

## 4. Experimental Evaluation

In the experiments, there were three signals from three different systems considered. The first system was the linear actuator DSZY1-24-05-A-050-IP65 and its voltage input signal. The second system was the incremental linear encoder L18-F10-0120-05-0-CP03/W with the displacement feedback. The third system was the KUKA iiwa R820 manipulator with the angular position feedback from its encoders.

The first signal was the analogue signal measured in volts, which was characterized by the noise described by the normal distribution $N(0, 0.001)$. The second signal was the displacement signal measured in mm, where the minimum incremental motion is 1.0 $\mu$m (accuracy grade at 1.0 m: 3.0 $\mu$m). The third signal corresponded to the angular position of a joint of the manipulator measured in degrees, where the minimum incremental motion was 3.0–4.0 $\mu$deg. Unfortunately, demonstrations of the filtering, fractional-order differentiation and integration based on the random signals (obtained from the described systems)

would be difficult due to the unknown fractional differentials and integrals of these signals. Therefore, the same signals (functions $f(t)$) were used as the base for the experimental evaluation, where the quality of each signal was described by noise and the observable minimum incremental motion characterizing each of the discussed systems.

Moreover, there were two types of tests conducted. In the first test, the ability to filter, differentiate and integrate based only on the local data was investigated. Then, in the second group of the tests, the ability of filtering, integer- and fractional-order differentiation, and integration with respect to the time base (globally), was evaluated. Frequency responses were not considered because the local (fractional) FIR differentiator/integrator frequency responses do not correspond to their equivalent theoretical responses. Furthermore, the time-variant FIR architecture eliminates the possibility of its analysis in the frequency domain.

In the first test, function $f(t) = t^2$ was used. This function was affected by the noise described by the distribution $N(0, 0.1)$. In this case, the noise was significantly (one hundred times) higher than in the first system. The sampling frequency of the test signal was 16384 Hz, while parameters of the first FIR architecture were $d = 0$, $N_f = 16384$, and $p_f = 2$. Hence, the FIR architecture estimated its output based on samples up to 1 s from the past. The results are presented in Figure 2.

In the first group of tests (Fig. 2), five different filtering (Fig. 2a), integer- (Fig. 2b) and fractional-order (Fig. 2c) differentiation, and fractional- (Fig. 2d) and integer-order (Fig. 2e) integration examples are presented. In all the cases, the output of the FIR architecture is in close range (based on visual inspection) to its corresponding theoretical function (its local differential and integral). However, the function $f(t)$ was not fitted to the data $f(t) + N(0, 0.1)$. Therefore, there is a noticeable difference between the outputs of the FIR architectures, and the function $f(t)$ and the corresponding theoretical differentials/ integrals. In this case, the recovery of the original signal $f(t)$ is a more demanding process than a local fit of this function with respect to the least squares-based regression. However, the output from the FIR filter (Fig. 2a) was 0.060% different from the output from the original signal f(t). In the case of the integer ($v = 1$, Fig. 2b) and the fractional ($v = 1/2$, Fig. 2c) differentiation, the differences between the responses from the FIR architecture and the corresponding theoretical differential $\frac{d^v f(t)}{dt^v}$ were 0.001% and 0.011%, respectively. In the case of the fractional ($v = -1/2$, Fig. 2d) and the integer ($v = -1$, Fig. 2e) integral, the differences between the responses from the FIR architecture and the corresponding integral values were 0.147% and 0.273%, respectively.

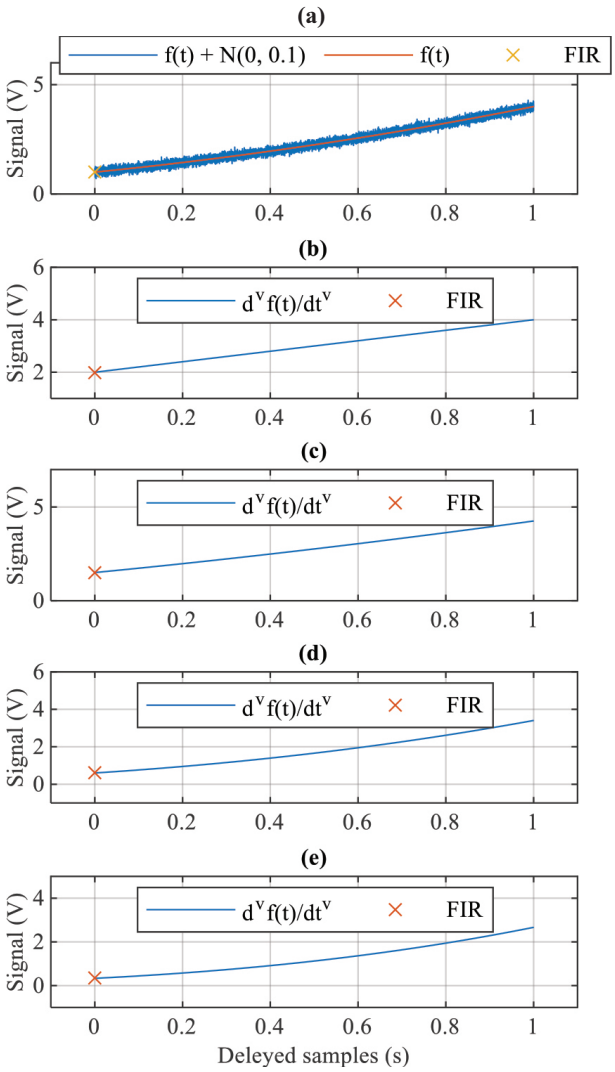


**Figure 2.** Comparison of different FIR architecture outputs during local differentiation and integration: (a) reference signal with and without noise compared to the FIR filter output; (b) ideal integer differential for $v = 1$ compared to the FIR differentiator output $v_f = 1$; (c) ideal fractional differential for $v = 1/2$ compared to the FIR differentiator output $v_f = 1/2$; (d) ideal fractional integral for $v = -1/2$ compared to the FIR integrator output $v_f = -1/2$; (e) ideal integer integral for $v = -1$ compared to the FIR integrator output $v_f = -1$.

The first FIR architecture designed with respect to (6)–(9) can provide only accurate responses based on the signal samples stored in the delay line of that FIR architecture. These responses are only true locally. Therefore, the proposed FIR architecture can work as a filter or an integer differentiator. Nevertheless, local fractional-differentiators and integer/fractional-integrators can also find a wide area of application. A perfect example is the fractional proportional-derivative-integral controller, where the responses of each of the controller's components can be estimated locally.

Moreover, the proposed FIR architecture introduces a negligible time delay into the closed-loop system. Thus, the small-phase-shift filtering has a positive impact on the response dynamics and stability of closed-loop control systems. Unfortunately, only the FIR filter and integer differentiator can be used for other purposes such as the real-time identification and disturbance observer design.

In the second group of tests, the function $f(t)$ was divided into three parts. In the first part, $f(t) = t^2$, $t \in (0, 30]$. In the second part, $f(t) = -40t + 2100$, $t \in (30, 60]$. In the third part, $f(t) = 0.2(t-75)3 + 374.9$, $t \in (60, 90]$.

These functions were chosen to create similar conditions for the FIR architectures such as (angular) velocity corresponding to the rate of the (angle) position change of the second and third system, and the voltage signal from the analogue controller output in the first system. The only exceptions are the discontinuous transitions between these functions. The first considered system is the linear actuator with noise described by the normal distribution $N(0, 0.001)$, that affected its voltage input signal. The results are presented in Figure 3.

The FIR architecture parameters used to obtain the results presented in Figure 3, were $d = 0$, $N_f = 40$, and $p_f = 1$ for the first time-invariant architecture, and $N_p = 4$ and $p_f = 3$ for the second time-variant FIR architecture. Moreover, the sampling frequency of the FIR architecture was reduced to 8 Hz. The sampling frequency of the input signal remained the same (16384 Hz). Again, five different output examples are discussed. The filtering results are presented in Figure 3a, the integer and fractional differentiation in Figure 3c and Figure 3d, and the fractional and integer integration in Figure 3e and Figure 3f, respectively.

Based on the results (Fig. 3), the output of the FIR architectures was in close range to the theoretical functions, and so were its global (fractional) differentials and integrals. As in the first test, no fitting was done to the data $f(t)+N(0, 0.001)$. In the cases of integer ($v = 1$, Fig. 3b) and fractional ($v = 1/2$, Fig. 3c) differentiation, the average absolute difference with respect to the maximum absolute value of the theoretical signal was 3.78% and 144%, respectively. Unfortunately, these average values were strongly affected by the errors appearing during the transition states between the functions. Therefore, the median was used to compare integer and fractional differentiation results. In this case, the median-based difference was reduced to 0.19% and 1.04%, respectively. In the case of integration, the average differences were comparable to those of fractional differentiation (178.36% and 188.46% for the fractional and integer integration, respectively), while the median differences were reduced to 1.19% and 1.10% for the fractional and integer integration.

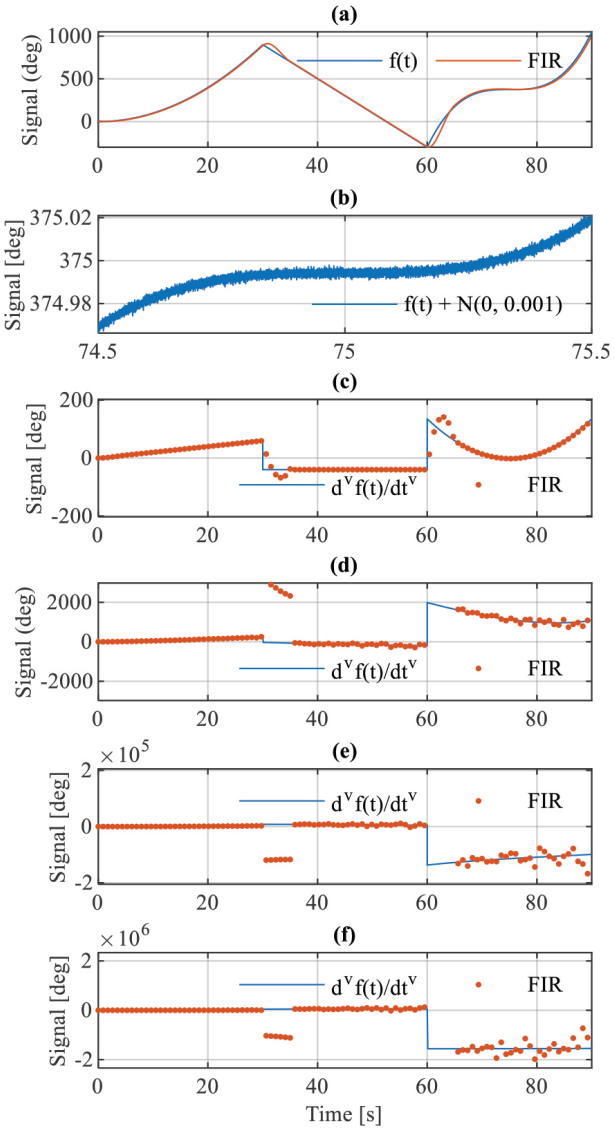


**Figure 3.** Comparison of different FIR architecture outputs during global differentiation and integration – analogue signal example: (a) reference signal with and without noise compared to the FIR filter output; (b) magnified (a) within $t \in [74.5, 75.5]$; (c) ideal integer differential for $v = 1$ compared to the FIR differentiator output $v_f = 1$; (d) ideal fractional differential for $v = 1/2$ compared to the FIR differentiator output $v_f = 1/2$; (e) ideal fractional integral for $v = -1/2$ compared to the FIR integrator output $v_f = -1/2$; (f) ideal integer integral for $v = -1$ compared to the FIR integrator output $v_f = -1$.

Comparable results and problems were observed when the fractional differentiation and integration were applied to the signal obtained from the digital encoder of the third system. The results are presented in Figure 4.

The FIR architecture parameters used to obtain the results presented in Figure 4, were $d = 0$, $N_f = 1000$, and $p_f = 2$ for the first time-invariant architecture, and $N_p = 4$, and $p_f = 3$ for the second time-variant FIR architecture. The sampling frequency of the FIR architecture was reduced to 4096 Hz. The sampling frequency of the input signal remained also the same

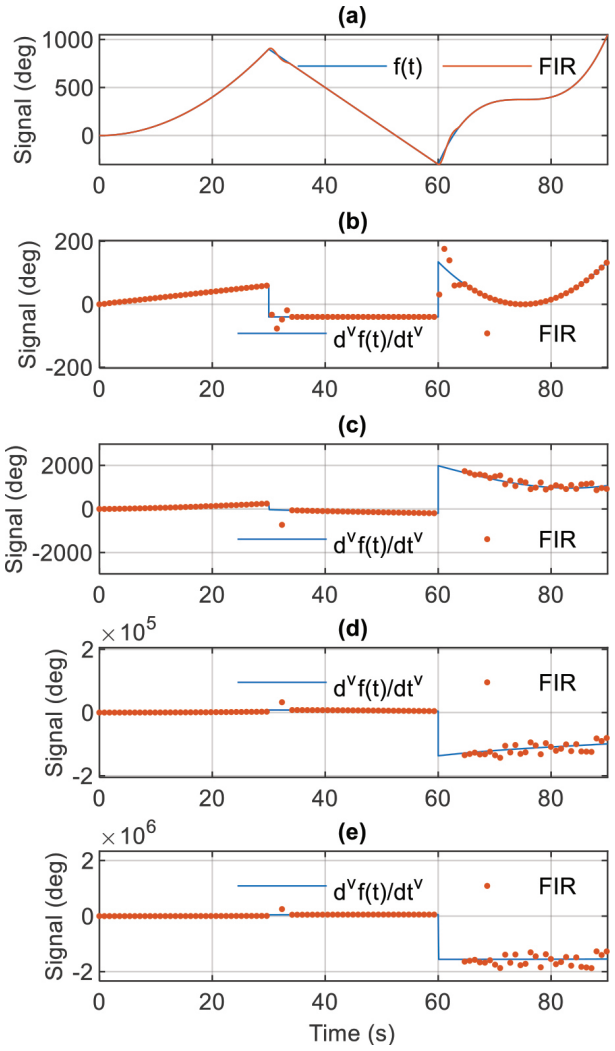


**Figure 4.** Comparison of different FIR architecture outputs during global differentiation and integration – digital encoder signal example: (a) reference signal with and without noise compared to the FIR filter output; (b) ideal integer differential for $v = 1$ compared to the FIR differentiator output $v_f = 1$; (c) ideal fractional differential for $v = 1/2$ compared to the FIR differentiator output $v_f = 1/2$; (d) ideal fractional integral for $v = -1/2$ compared to the FIR integrator output $v_f = -1/2$; and (e) ideal integer integral for $v = -1$ compared to the FIR integrator output $v_f = -1$.

(16384 Hz). Again, in the case of the signal from the digital encoder of the third system, filtering results are presented in Figure 4a, integer and fractional differentiation in Figure 4c and Figure 4d, and fractional and integer integration in Figure 4e and Figure 4f, respectively.

Based on the results presented in Figure 4, the output of the FIR architectures was also comparable to the theoretical functions corresponding to the global (fractional and integer) differentials and integrals. The integer ($v = 1$, Figure 4b) and fractional ($v = 1/2$, Figure 4c) differentiation results were characterized by an average difference of 2.09% and 435.00%, respectively. Again, this average indicator was strongly affected by the errors appearing during the transition states between the functions. Hence, the median-based difference was reduced to 0.000016% and 0.010% for the integer and fractional differentiation, respectively. The average differences corresponding to the fractional and integer integration were 526.87% and 554.31%, while the equivalent median differences were reduced to 0.04% and 0.02%, respectively.

The same tests were conducted with respect to the second system, where the observable minimum incremental motion was at the level of a single micrometer. In this case, however, the FIR architectures required a drastic reduction of the sampling frequency, which was reduced to 4 Hz. The remaining FIR architecture parameters were $d = 0$, $N_f = 40$, and $p_f = 2$ for the first time-invariant architecture, and $N_p = 4$, and $p_f = 3$ for the second time-variant FIR architecture. The rest of the parameters and conditions remained the same as in the two preceding experiments.

In the case of the integer ($v = 1$) and fractional ($v = 1/2$) differentiation, the average difference was 4.84 % and 145.92%, while the median difference was 0.37% and 0.12%, respectively. The average differences corresponding to the fractional and integer integration were 183.81% and 197.19%, while the corresponding median differences were 0.06% and 0.04%, respectively.

Unfortunately, fractional differentiation combines differentiation and integration. Therefore, this process is extremely sensitive to noise because the corresponding error increases in each computation cycle in the FIR architecture. Nevertheless, by reducing the sampling frequency of the first FIR architecture more attenuation was achieved for the stopband frequency of this architecture. Thus, it provided a better filtered data set for the second time-variant FIR architecture.

The time delay introduced to the method of design of the proposed FIR architecture significantly increased the attenuation of the stopband frequency of the first FIR filter. However, this delay also introduced a phase shift to the filtered signal. In result, it drastically increased the error of the estimated output. Hence, the reduction of the sampling frequency turned out to be a better solution to increase attenuation of the proposed FIR architecture than introduction of a delay to that architecture. Nevertheless, fractional differentiation and integration require an extreme level of attenuation for the stopband frequency which was a challenge for the proposed solution. In this case, the parameters of each of the discussed FIR architectures were set according to visual inspection of their responses. There are therefore two challenges for this solution, which are increasing the attenuation of the stopband frequency and optimizing the FIR architecture parameters.

Moreover, adaptation of the proposed design method into an IIR digital architecture could solve the problems of the numerical errors and the required time base. However, it is not a trivial task due to the adaptation of the method of least squares into the

design method of the proposed FIR architecture and the stability problems of an IIR digital system.

## 5. Conclusion

In this paper, the design method, and the time-variant FIR architecture for real-time estimation of local and global fractional and integer differentiators and integrators were presented. The proposed FIR architecture was divided into two parts. In the first part, the FIR architecture was time-invariant, while in the second part, the parameters of the architecture were estimated with respect to the time base. The separation into two independent parts was necessary because a single time-variant FIR architecture would require real-time matrix inversion or extensive analytical solutions. The matrix inversion in the design method was critical to ensure small delay (phase shift) caused by each of the FIR architectures. The small delay resulted from the optimum output obtained with respect to the method of least squares. Unfortunately, there are limitations of the proposed solution. The first limitation is the limited ability to approximate the input signal by the time-variant FIR architecture, while the second limitation is strictly related to the numerical errors. Moreover, since fractional differentiation combines differentiation and integration, this process is extremely sensitive to the noise and the limited resolution of the measurements. However, by reducing the sampling frequency of the first FIR architecture or increasing its order, more attenuation can be achieved for the stopband frequency of the proposed FIR architecture. Furthermore, despite these limitations, there are systems oriented on closed-loop control, disturbance observations and real-time identification of model parameters, where the proposed solution can be implemented.

**AUTHOR**

**Mateusz Saków*** – Research Institute of Signals, Sensors and Systems, School of Engineering & Physical Sciences, Heriot-Watt University, Edinburgh, UK EH14 4AS, Scotland, UK, e-mail: sakow.mat@gmail.com.

*Corresponding author

## References

[1] K. Oldham and J. Spanier, *The fractional calculus theory and applications of differentiation and integration to arbitrary order*. Elsevier, 1974.

[2] H. Sun, Y. Zhang, D. Baleanu, W. Chen, and Y. Chen, "A new collection of real world applications of fractional calculus in science and engineering," *Communications in Nonlinear Science and Numerical Simulation*, vol. 64, pp. 213–231, 2018.

[3] I. Petráš, *Fractional-order nonlinear systems: modeling, analysis and simulation*. Springer Science & Business Media, 2011.

[4] J. D. Colín-Cervantes et al., "Rational approximations of arbitrary order: A survey," *Fractal and Fractional*, vol. 5, no. 4, p. 267, 2021.

[5] B. T. Krishna, "Studies on fractional order differentiators and integrators: A survey," *Signal processing*, vol. 91, no. 3, pp. 386–426, 2011.

[6] L. Debnath, "Recent applications of fractional calculus to science and engineering," *International Journal of Mathematics and Mathematical Sciences*, vol. 2003, no. 54, pp. 3413–3442, 2003.

[7] S. Manabe, "The non-integer integral and its application to control systems," *Mitsubishi Denki laboratory reports*, vol. 2, no. 2, 1961.

[8] M. Axtell and M. E. Bise, "Fractional calculus application in control systems," in *IEEE conference on aerospace and electronics*, 1990: IEEE, pp. 563–566.

[9] W. Jifeng and L. Yuankai, "Frequency domain analysis and applications for fractional-order control systems," in *Journal of physics: Conference series*, 2005, vol. 13, no. 1: IOP Publishing, p. 268.

[10] A. Charef, "Analogue realisation of fractional-order integrator, differentiator and fractional PI$\lambda$D$\mu$ controller," *IEE Proceedings-Control Theory and Applications*, vol. 153, no. 6, pp. 714–720, 2006.

[11] N. Ferreira, F. Duarte, M. Lima, M. Marcos, and J. Machado, "Application of fractional calculus in the dynamical analysis and control of mechanical manipulators," *Fractional calculus and applied analysis*, vol. 11, no. 1, pp. 91–113, 2008.

[12] J. Tenreiro Machado and A. Galhano, "A new method for approximating fractional derivatives: application in non-linear control," *ENOC-2008*, pp. 1–5, 2008.

[13] J. Mocak, I. Janiga, M. Rievaj, and D. Bustin, "The use of fractional differentiation or integration for signal improvement," *Measurement Science Review*, vol. 7, no. 5, pp. 39–42, 2007.

[14] G. Li, Y. Li, H. Chen, and W. Deng, "Fractional-order controller for course-keeping of underactuated surface vessels based on frequency domain specification and improved particle swarm optimization algorithm," *Applied Sciences*, vol. 12, no. 6, p. 3139, 2022.

[15] M. Shitikova, "Fractional operator viscoelastic models in dynamic problems of mechanics of solids: A review," *Mechanics of solids*, pp. 1–33, 2022.

[16] F. Özköse, M. Yavuz, M. T. Şenel, and R. Habbireeh, "Fractional order modelling of omicron SARS-CoV-2 variant containing heart attack effect using real data from the United Kingdom," *Chaos, Solitons & Fractals*, vol. 157, p. 111954, 2022.

[17] X. Zhang, G. Yang, S. Liu, and A. J. Moshayedi, "Fractional-order circuit design with hybrid controlled memristors and FPGA implementation,"

*AEU-International Journal of Electronics and Communications*, vol. 153, p. 154268, 2022.

[18] P. Bertsias, S. Kapoulea, C. Psychalinos, and A. S. Elwakil, "A collection of interdisciplinary applications of fractional-order circuits," in *Fractional Order Systems*: Elsevier, 2022, pp. 35–69.

[19] M. Joshi, S. Bhosale, and V. A. Vyawahare, "A survey of fractional calculus applications in artificial neural networks," *Artificial Intelligence Review*, pp. 1–54, 2023.

[20] E. Yumuk, M. Güzelkaya, and İ. Eksin, "A robust fractional-order controller design with gain and phase margin specifications based on delayed Bode's ideal transfer function," *Journal of the Franklin Institute*, vol. 359, no. 11, pp. 5341–5353, 2022.

[21] G. Gembalczyk, P. Gierlak, and S. Duda, "Modeling and control of an underactuated system for dynamic body weight support," *Applied Sciences*, vol. 11, no. 3, p. 905, 2021.

[22] G. Gembalczyk, P. Domogała, and K. Leśniowski, "Modeling of Underactuated Ball and Beam System—A Comparative Study," in *Actuators*, 2023, vol. 12, no. 2: MDPI, p. 59.

[23] Y. Wang, G. Wang, G. Yao, and L. Shen, "Research on the Characteristics of Operating Non-Uniformity of a High-Pressure Common-Rail Diesel Engine Based on Crankshaft Segment Signals," *IEEE Access*, vol. 9, pp. 64906–64917, 2021.

[24] M. Sugi and K. Saito, "Non-integer exponents in electronic circuits: F-matrix representation of the power-law conductivity," *IEICE TRANSACTIONS on Fundamentals of Electronics, Communications and Computer Sciences*, vol. 75, no. 6, pp. 720–725, 1992.

[25] I. Podlubny, I. Petráš, B. M. Vinagre, P. O'Leary, and Ľ. Dorčák, "Analogue realizations of fractional-order controllers," *Nonlinear dynamics*, vol. 29, pp. 281–296, 2002.

[26] B. Krishna and K. Reddy, "Analysis of fractional order low pass and high pass filters," *Journal of Electrical Engineering*, vol. 8, no. 1, pp. 4–4, 2008.

[27] M. Koseoglu, F. N. Deniz, B. B. Alagoz, and H. Alisoy, "An effective analog circuit design of approximate fractional-order derivative models of M-SBL fitting method," *Engineering Science and Technology, an International Journal*, vol. 33, p. 101069, 2022.

[28] Z. M. Shah, M. Y. Kathjoo, F. A. Khanday, K. Biswas, and C. Psychalinos, "A survey of single and multi-component Fractional-Order Elements (FOEs) and their applications," *Microelectronics Journal*, vol. 84, pp. 9–25, 2019.

[29] M. E. Van Valkenburg, "Introduction to modern network synthesis,", 1960.

[30] M. Saków and K. Marchelek, "Design and optimisation of regression-type small phase shift FIR filters and FIR-based differentiators with optimal local response in LS-sense," *Mechanical Systems and Signal Processing*, vol. 152, p. 107408, 2021.

[31] R. Karthick, A. Senthilselvi, P. Meenalochini, and S. Senthil Pandi, "Design and analysis of linear phase finite impulse response filter using water strider optimization algorithm in FPGA," *Circuits, Systems, and Signal Processing*, vol. 41, no. 9, pp. 5254–5282, 2022.

[32] F. Arellano-Espitia, M. Delgado-Prieto, A.-D. Gonzalez-Abreu, J. J. Saucedo-Dorantes, and R. A. Osornio-Rios, "Deep-Compact-Clustering based anomaly detection applied to electromechanical industrial systems," *Sensors*, vol. 21, no. 17, p. 5830, 2021.

[33] Y. Zhou et al., "Transient measurement of mechatronic multi-parameters and kinetics performances for linear piezoelectric motors," *Measurement*, vol. 203, p. 112032, 2022.

[34] D. P. Atherton, N. Tan, and A. Yüce, "Methods for computing the time response of fractional-order systems," *IET Control Theory & Applications*, vol. 9, no. 6, pp. 817–830, 2015.

[35] C. Hwang, J.-F. Leu, and S.-Y. Tsay, "A note on time-domain simulation of feedback fractional-order systems," *IEEE Transactions on Automatic Control*, vol. 47, no. 4, pp. 625–631, 2002.

[36] R. S. Barbosa, J. T. Machado, and I. M. Ferreira, "Tuning of PID controllers based on Bode's ideal transfer function," *Nonlinear dynamics*, vol. 38, pp. 305–321, 2004.

[37] A. Oustaloup, F. Levron, B. Mathieu, and F. M. Nanot, "Frequency-band complex noninteger differentiator: characterization and synthesis," *IEEE Transactions on Circuits and Systems I: Fundamental Theory and Applications*, vol. 47, no. 1, pp. 25–39, 2000.

[38] D. Xue, C. Zhao, and Y. Chen, "A modified approximation method of fractional order system," in *2006 international conference on mechatronics and automation*, 2006: IEEE, pp. 1043–1048.

[39] A. Charef, H. Sun, Y. Tsao, and B. Onaral, "Fractal system as represented by singularity function," *IEEE Transactions on Automatic Control*, vol. 37, no. 9, pp. 1465–1470, 1992.

[40] G. Carlson and C. Halijak, "Approximation of fractional capacitors (1/s)^(1/n) by a regular Newton process," *IEEE Transactions on Circuit Theory*, vol. 11, no. 2, pp. 210–213, 1964.

[41] F. MatsudaK, "H (infinity) optimized wave-absorbing control-Analytical and experimental results," *Journal of Guidance, Control, and Dynamics*, vol. 16, no. 6, p. 1146–1153, 1993.

[42] A. N. Khovanskii, The application of continued fractions and their generalizations to problems in approximation theory. Noordhoff Groningen, 1963.

[43] K. Bingi, R. Ibrahim, M. N. Karsiti, S. M. Hassam, and V. R. Harindran, "Frequency response based curve fitting approximation of fractional-order PID controllers," *International Journal of Applied Mathematics and Computer Science*, vol. 29, no. 2, pp. 311–326, 2019.

[44] K. Bingi, R. Ibrahim, M. N. Karsiti, S. M. Hassan, and V. R. Harindran, *Fractional-order systems and PID controllers*. Springer, 2020.

[45] C. Sanathanan and J. Koerner, "Transfer function synthesis as a ratio of two complex polynomials," *IEEE transactions on automatic control*, vol. 8, no. 1, pp. 56–58, 1963.

[46] F. N. Deniz, B. B. Alagoz, N. Tan, and M. Koseoglu, "Revisiting four approximation methods for fractional order transfer function implementations: Stability preservation, time and frequency response matching analyses," *Annual Reviews in Control*, vol. 49, pp. 239–257, 2020.

[47] B. Gustavsen and A. Semlyen, "Rational approximation of frequency domain responses by vector fitting," *IEEE Transactions on power delivery*, vol. 14, no. 3, pp. 1052–1061, 1999.

[48] A. Djouambi, A. Charef, and A. Besançon, "Optimal approximation, simulation and analog realization of the fundamental fractional order transfer function," *International Journal of Applied Mathematics and Computer Science*, vol. 17, no. 4, pp. 455–462, 2007.

[49] G. Maione, "Continued fractions approximation of the impulse response of fractional-order dynamic systems," *IET Control Theory & Applications*, vol. 2, no. 7, pp. 564–572, 2008.

[50] G. Maione, "Closed-form rational approximations of fractional, analog and digital differentiators/integrators," *IEEE journal on emerging and selected topics in circuits and systems*, vol. 3, no. 3, pp. 322–329, 2013.

[51] C.-C. Tseng, "Design of fractional order digital FIR differentiators," *IEEE Signal processing letters*, vol. 8, no. 3, pp. 77–79, 2001.

[52] Ľ. Dorèák, J. Terpák, I. Petráš, and F. Dorèáková, "Electronic realization of the fractional-order systems," *Acta Montanistica Slovaca*, vol. 12, no. 3, pp. 231–237, 2007.

[53] Y. Chen and B. M. Vinagre, "A new IIR-type digital fractional order differentiator," *Signal processing*, vol. 83, no. 11, pp. 2359–2365, 2003.

[54] B. M. Vinagre, Y. Q. Chen, and I. Petráš, "Two direct Tustin discretization methods for fractional-order differentiator/integrator," *Journal of the franklin institute*, vol. 340, no. 5, pp. 349–362, 2003.

[55] M. Aoun, R. Malti, F. Levron, and A. Oustaloup, "Numerical simulations of fractional systems: an overview of existing methods and improvements," *Nonlinear Dynamics*, vol. 38, pp. 117–131, 2004.

[56] G. Maione, "A digital, noninteger order, differentiator using laguerre orthogonal sequences," *International Journal of Intelligent Control and Systems*, vol. 11, no. 2, pp. 77–81, 2006.

[57] A. Djouambi, A. Charef, and A. V. Besançon, "Approximation and synthesis of non integer order systems," *IFAC Proceedings Volumes*, vol. 39, no. 11, pp. 265–268, 2006.

[58] J. T. Machado, "Analysis and design of fractional-order digital control systems," *Systems Analysis Modelling Simulation*, vol. 27, no. 2-3, pp. 107–122, 1997.

[59] B. Krishna and K. Reddy, "Design of fractional order digital differentiators and integrators using indirect discretization," *Fractional Calculus and applied analysis*, vol. 11, no. 2, pp. 143p-151p, 2008.

[60] B. Krishna and K. Reddy, "Design of digital differentiators and integrators of order," *World Journal of Modelling and Simulation*, vol. 4, no. 3, pp. 182–187, 2008.

[61] M. A. Al-Alaoui, "Novel approach to designing digital differentiators," *Electronics Letters*, vol. 28, no. 15, pp. 1376–1378, 1992.

[62] M. A. Al-Alaoui, "Novel digital integrator and differentiator," *Electronics letters*, vol. 29, no. 4, pp. 376–378, 1993.

[63] J. Le Bihan, "Novel class of digital integrators and differentiators," *Electronics Letters*, vol. 29, no. 11, pp. 971–973, 1993.

[64] M. A. Al-Alaoui, "Novel IIR differentiator from the Simpson integration rule," *IEEE Transactions on Circuits and Systems I: Fundamental Theory and Applications*, vol. 41, no. 2, pp. 186–187, 1994.

[65] M. A. Al-Alaoui, "Filling the gap between the bilinear and the backward-difference transforms: an interactive design approach," *International Journal of Electrical Engineering Education*, vol. 34, no. 4, pp. 331–337, 1997.

[66] M. A. Al-Alaoui, "Novel stable higher order s-to-z transforms," *IEEE Transactions on Circuits and Systems I: Fundamental Theory and Applications*, vol. 48, no. 11, pp. 1326–1329, 2001.

[67] A.-A. M. Al, "Al-Alaoui operator and the $\alpha$-approximation for discretization analog systems," *Facta universitatis-series: Electronics and Energetics*, vol. 19, no. 1, pp. 143–146, 2006.

[68] N. Q. Ngo, "A new approach for the design of wideband digital integrator and differentiator," *IEEE Transactions on Circuits and Systems II: Express Briefs*, vol. 53, no. 9, pp. 936–940, 2006.

[69] M. A. Al-Alaoui, "Novel approach to analog-to-digital transforms," *IEEE Transactions on Circuits and Systems I: Regular Papers*, vol. 54, no. 2, pp. 338–350, 2007.

[70] M. Sakow and K. Marchelek, "Design and optimisation of regression-type small phase shift FIR

filters and FIR-based differentiators with optimal local response in LS-sense," *Mechanical Systems and Signal Processing*, vol. 152, p. 107408, 2021.

[71] D. Cafagna and G. Grassi, "Fractional-order Chua's circuit: time-domain analysis, bifurcation, chaotic behavior and test for chaos," *International Journal of Bifurcation and Chaos*, vol. 18, no. 03, pp. 615–639, 2008.

[72] A. Dabiri and E. A. Butcher, "Numerical solution of multi-order fractional differential equations with multiple delays via spectral collocation methods," *Applied Mathematical Modelling*, vol. 56, pp. 424–448, 2018.

[73] A. Dabiri and E. A. Butcher, "Stable fractional Chebyshev differentiation matrix for the numerical solution of multi-order fractional differential equations," *Nonlinear Dynamics*, vol. 90, pp. 185–201, 2017.

[74] K. Diethelm, N. J. Ford, and A. D. Freed, "A predictor-corrector approach for the numerical solution of fractional differential equations," *Nonlinear Dynamics*, vol. 29, pp. 3–22, 2002.

[75] W. Deng, "Numerical algorithm for the time fractional Fokker–Planck equation," *Journal of Computational Physics*, vol. 227, no. 2, pp. 1510–1522, 2007.

[76] C. Li, J. Xiong, W. Li, Y. Tong, and Y. Zeng, "Robust synchronization for a class of fractional-order dynamical system via linear state variable," *Indian Journal of Physics*, vol. 87, pp. 673–678, 2013.

[77] M. Saków and K. Marchelek, "Model-free and time-constant prediction for closed-loop systems with time delay," *Control Engineering Practice*, vol. 81, pp. 1–8, 2018.

[78] M. Saków, "Novel robust disturbance observer," *ISA transactions*, vol. 104, pp. 255–277, 2020.

[79] Y. Cui, H. Sun, and L. Hou, "Decentralized event-triggered adaptive neural network control for nonstrict-feedback nonlinear interconnected systems with external disturbances against intermittent DoS attacks," *Neurocomputing*, vol. 517, pp. 133–147, 2023.

[80] D. T. Tena, "Design of disturbance observers based on their implementability in industrial control systems," Universitat Jaume I, 2022.

[81] D. Tena, I. Peñarrocha-Alós, and R. Sanchis, "Performance, robustness and noise amplification trade-offs in Disturbance Observer Control design," *European Journal of Control*, vol. 65, p. 100630, 2022.

[82] N. Fink, G. Zenan, P. Szemes, and P. Korondi, "Comparison of Direct and Inverse Model-based Disturbance Observer for a Servo Drive System," *Acta Polytechnica Hungarica*, vol. 20, no. 4, 2023.

[83] V. L. Korupu and M. Muthukumarasamy, "A comparative study of various Smith predictor configurations for industrial delay processes," *Chemical Product and Process Modeling*, vol. 17, no. 6, pp. 701–732, 2021.

[84] S. Chen, W. Xue, and Y. Huang, "Analytical design of active disturbance rejection control for nonlinear uncertain systems with delay," *Control Engineering Practice*, vol. 84, pp. 323–336, 2019.

[85] S. Guo, Y. Liu, Y. Zheng, and T. Ersal, "A Delay Compensation Framework for Connected Testbeds," *IEEE Transactions on Systems, Man, and Cybernetics: Systems*, vol. 52, no. 7, pp. 4163–4176, 2021.